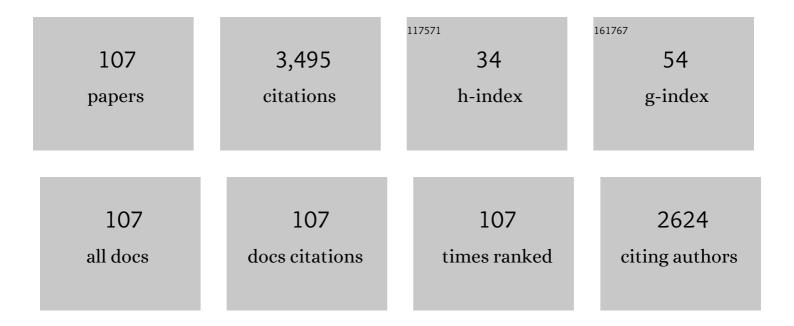
List of Publications by Year in descending order

Source: https://exaly.com/author-pdf/8737849/publications.pdf Version: 2024-02-01



#	Article	IF	CITATIONS
1	Two-Dimensional Covalent Organic Frameworks with Cobalt(II)-Phthalocyanine Sites for Efficient Electrocatalytic Carbon Dioxide Reduction. Journal of the American Chemical Society, 2021, 143, 7104-7113.	6.6	198
2	High Performance Organic Field-Effect Transistors Based on Amphiphilic Tris(phthalocyaninato) Rare Earth Triple-Decker Complexes. Journal of the American Chemical Society, 2005, 127, 15700-15701.	6.6	194
3	Morphology Controlled Self-Assembled Nanostructures of Sandwich Mixed (Phthalocyaninato)(Porphyrinato) Europium Triple-Deckers. Effect of Hydrogen Bonding on Tuning the Intermolecular Interaction. Journal of the American Chemical Society, 2008, 130, 11623-11630.	6.6	146
4	Highâ€Performance Airâ€Stable Ambipolar Organic Fieldâ€Effect Transistor Based on Tris(phthalocyaninato) Europium(III). Advanced Materials, 2012, 24, 1755-1758.	11.1	111
5	Facile approaches to build ordered amphiphilic tris(phthalocyaninato) europium triple-decker complex thin films and their comparative performances in ozone sensing. Physical Chemistry Chemical Physics, 2010, 12, 12851.	1.3	106
6	Facile preparation of N-doped corncob-derived carbon nanofiber efficiently encapsulating Fe2O3 nanocrystals towards high ORR electrocatalytic activity. Journal of Energy Chemistry, 2020, 44, 121-130.	7.1	100
7	In situ construction of Co/N/C-based heterojunction on biomass-derived hierarchical porous carbon with stable active sites using a Co-N protective strategy for high-efficiency ORR, OER and HER trifunctional electrocatalysts. Journal of Energy Chemistry, 2021, 54, 626-638.	7.1	92
8	Maximizing Electroactive Sites in a Threeâ€Dimensional Covalent Organic Framework for Significantly Improved Carbon Dioxide Reduction Electrocatalysis. Angewandte Chemie - International Edition, 2022, 61, .	7.2	83
9	Efficient ORR electrocatalytic activity of peanut shell-based graphitic carbon microstructures. Journal of Materials Chemistry A, 2018, 6, 12018-12028.	5.2	81
10	An ultrafast responsive NO ₂ gas sensor based on a hydrogen-bonded organic framework material. Chemical Communications, 2020, 56, 703-706.	2.2	77
11	Differential study of substituted and unsubstituted cobalt phthalocyanines for gas sensor applications. Sensors and Actuators B: Chemical, 2011, 159, 163-170.	4.0	70
12	Self-assembled aggregates of amphiphilic perylene diimide–based semiconductor molecules: Effect of morphology on conductivity. Journal of Colloid and Interface Science, 2012, 368, 387-394.	5.0	69
13	Thin-Film Transistors Based on Langmuirâ^'Blodgett Films of Heteroleptic Bis(phthalocyaninato) Rare Earth Complexes. Langmuir, 2005, 21, 6527-6531.	1.6	68
14	Synthesis, Characterization, and OFET Properties of Amphiphilic Heteroleptic Tris(phthalocyaninato) Europium(III) Complexes with Hydrophilic Poly(oxyethylene) Substituents. Inorganic Chemistry, 2007, 46, 11397-11404.	1.9	68
15	Air-stable ambipolar field-effect transistor based on a solution-processed octanaphthoxy-substituted tris(phthalocyaninato) europium semiconductor with high and balanced carrier mobilities. Chemical Science, 2015, 6, 1967-1972.	3.7	68
16	Amphiphilic Perylenetretracarboxyl Diimide Dimer and Its Application in Field Effect Transistor. Langmuir, 2007, 23, 5836-5842.	1.6	66
17	Nonperipherally Octa(butyloxy)‣ubstituted Phthalocyanine Derivatives with Good Crystallinity: Effects of Metal–Ligand Coordination on the Molecular Structure, Internal Structure, and Dimensions of Selfâ€Assembled Nanostructures. Chemistry - A European Journal, 2009, 15, 13241-13252.	1.7	66
18	The cobalt carbide/bimetallic CoFe phosphide dispersed on carbon nanospheres as advanced bifunctional electrocatalysts for the ORR, OER, and rechargeable Zn–air batteries. Journal of Colloid and Interface Science, 2021, 590, 321-329.	5.0	66

#	Article	IF	CITATIONS
19	Effect of Peripheral Hydrophobic Alkoxy Substitution on the Organic Field Effect Transistor Performance of Amphiphilic Tris(phthalocyaninato) Europium Triple-Decker Complexes. Langmuir, 2007, 23, 12549-12554.	1.6	64
20	Amphiphilic (Phthalocyaninato) (Porphyrinato) Europium Triple-Decker Nanoribbons with Air-Stable Ambipolar OFET Performance. ACS Applied Materials & Interfaces, 2016, 8, 6174-6182.	4.0	55
21	Morphology and chirality controlled self-assembled nanostructures of porphyrin–pentapeptide conjugate: effect of the peptide secondary conformation. Journal of Materials Chemistry, 2011, 21, 8057.	6.7	54
22	Introduction of Multifunctional Triphenylamino Derivatives at the Perovskite/HTL Interface To Promote Efficiency and Stability of Perovskite Solar Cells. ACS Applied Materials & Interfaces, 2020, 12, 9300-9306.	4.0	53
23	Tuning the semiconducting nature of bis(phthalocyaninato) holmium complexes via peripheral substituents. Journal of Materials Chemistry, 2012, 22, 22142.	6.7	51
24	(TFPP)Eu[Pc(OPh) ₈]Eu[Pc(OPh) ₈]/CuPc Two-Component Bilayer Heterojunction-Based Organic Transistors with High Ambipolar Performance. ACS Applied Materials & Interfaces, 2015, 7, 2486-2493.	4.0	48
25	H-aggregation mode in triple-decker phthalocyaninato-europium semiconductors. Materials design for high-performance air-stable ambipolar organic thin film transistors. Organic Electronics, 2013, 14, 2582-2589.	1.4	46
26	Strategic design of cellulose nanofibers@zeolitic imidazolate frameworks derived mesoporous carbon-supported nanoscale CoFe2O4/CoFe hybrid composition as trifunctional electrocatalyst for Zn-air battery and self-powered overall water-splitting. Journal of Power Sources, 2022, 521, 230925.	4.0	45
27	The first solution-processable n-type phthalocyaninato copper semiconductor: tuning the semiconducting nature via peripheral electron-withdrawing octyloxycarbonyl substituents. Journal of Materials Chemistry, 2011, 21, 18552.	6.7	44
28	A Br-regulated transition metal active-site anchoring and exposure strategy in biomass-derived carbon nanosheets for obtaining robust ORR/HER electrocatalysts at all pH values. Journal of Materials Chemistry A, 2019, 7, 27089-27098.	5.2	40
29	Solution-processed thin films based on sandwich-type mixed (phthalocyaninato)(porphyrinato) europium triple-deckers: Structures and comparative performances in ammonia sensing. Sensors and Actuators B: Chemical, 2012, 166-167, 500-507.	4.0	39
30	Enhanced chemosensing of ammonia based on the novel molecular semiconductor-doped insulator (MSDI) heterojunctions. Sensors and Actuators B: Chemical, 2011, 155, 165-173.	4.0	38
31	The lower rather than higher density charge carrier determines the NH ₃ -sensing nature and sensitivity of ambipolar organic semiconductors. Materials Chemistry Frontiers, 2018, 2, 1009-1016.	3.2	38
32	An active site pre-anchoring and post-exposure strategy in Fe(CN)64-@PPy derived Fe/S/N-doped carbon electrocatalyst for high performance oxygen reduction reaction and zinc-air batteries. Chemical Engineering Journal, 2021, 413, 127395.	6.6	38
33	High-sensitive room-temperature NO2 sensor based on a soluble n-type phthalocyanine semiconductor. Inorganic Chemistry Communication, 2017, 77, 18-22.	1.8	36
34	Morphology Controlled Surface-Assisted Self-Assembled Microtube Junctions and Dendrites of Metal Free Porphyrin-Based Semiconductor. Langmuir, 2010, 26, 3678-3684.	1.6	35
35	N-channel organic thin-film transistors based on a soluble cyclized perylene tetracarboxylic diimide dimer. Organic Electronics, 2013, 14, 1197-1203.	1.4	35
36	(Pc)Eu(Pc)Eu[<i>trans</i> -T(COOCH ₃) ₂ PP]/GO Hybrid Film-Based Nonenzymatic H ₂ O ₂ Electrochemical Sensor with Excellent Performance. ACS Applied Materials & Interfaces, 2016, 8, 30398-30406.	4.0	35

#	Article	IF	CITATIONS
37	Aggregation Behavior of Heteroleptic Tris(phthalocyaninato) Dysprosium Complexes with Different Alkoxy Chains in Monolayer or Multilayer Solid Films. Langmuir, 2005, 21, 11289-11295.	1.6	34
38	Synthesis, Characterization and OFET Properties of Amphiphilic Mixed (Phthalocyaninato)(porphyrinato)europium(III) Complexes. European Journal of Inorganic Chemistry, 2009, 2009, 954-960.	1.0	34
39	In-situ growth of ZnS/FeS heterojunctions on biomass-derived porous carbon for efficient oxygen reduction reaction. Journal of Energy Chemistry, 2020, 47, 79-85.	7.1	32
40	Binuclear Phthalocyanine Dimerâ€Containing Yttrium Doubleâ€Decker Ambipolar Semiconductor with Sensitive Response toward Oxidizing NO ₂ and Reducing NH ₃ . ChemElectroChem, 2018, 5, 605-609.	1.7	31
41	A high-performance photoelectrochemical sensor for the specific detection of H ₂ O ₂ and glucose based on an organic conjugated microporous polymer. Journal of Materials Chemistry A, 2021, 9, 26216-26225.	5.2	31
42	Maximizing Electroactive Sites in a Threeâ€dimensional Covalent Organic Framework for Significantly Improved Carbon Dioxide Reduction Electrocatalysis. Angewandte Chemie, 0, , .	1.6	30
43	A perylenediimide modified SiO2@TiO2 yolk-shell light-responsive nanozyme: Improved peroxidase-like activity for H2O2 and sarcosine sensing. Journal of Hazardous Materials, 2022, 436, 129321.	6.5	29
44	Synthesis, self-assembly, and semiconducting properties of phenanthroline-fused phthalocyanine derivatives. Journal of Materials Chemistry, 2012, 22, 15695.	6.7	28
45	High Sensitive Ambipolar Response towards Oxidizing NO ₂ and Reducing NH ₃ Based on Bis(phthalocyaninato) Europium Semiconductors. Chinese Journal of Chemistry, 2016, 34, 975-982.	2.6	28
46	Two‣tep Solutionâ€Processed Twoâ€Component Bilayer Phthalocyaninato Copperâ€Based Heterojunctions with Interesting Ambipolar Organic Transiting and Ethanol‣ensing Properties. Advanced Materials Interfaces, 2016, 3, 1600253.	1.9	26
47	Polymorphism in the self-assembled nanostructures of a tris(phthalocyaninato) europium derivative: Phase-dependent semiconducting and NO2 sensing behaviour. Organic Electronics, 2018, 53, 127-134.	1.4	26
48	Novel heteroatom sulfur porphyrin organic polymer as a metal-free electrocatalyst for acidic oxygen reduction reaction. Electrochimica Acta, 2021, 377, 138107.	2.6	26
49	Solution-processed single crystal microsheets of a novel dimeric phthalocyanine-involved triple-decker for high-performance ambipolar organic field effect transistors. Chemical Communications, 2017, 53, 12754-12757.	2.2	25
50	Optimizing the gas sensing properties of sandwich-type phthalocyaninato europium complex through extending the conjugated framework. Dyes and Pigments, 2019, 161, 240-246.	2.0	25
51	A sandwich mixed (phthalocyaninato) (porphyrinato) europium triple-decker: Balanced-mobility, ambipolar organic thin-film transistor. Inorganic Chemistry Communication, 2014, 39, 79-82.	1.8	24
52	Effects of aromatic substituents on the electronic structure and excited state energy levels of diketopyrrolopyrrole derivatives for singlet fission. Physical Chemistry Chemical Physics, 2018, 20, 22997-23006.	1.3	24
53	High-performance ambipolar responses to oxidizing NO ₂ and reducing NH ₃ based on the self-assembled film of an amphiphilic tris(phthalocyaninato) europium complex. New Journal of Chemistry, 2017, 41, 11955-11961.	1.4	23
54	Porphyrinâ€₽OSS Molecular Hybrids. Chemistry - A European Journal, 2013, 19, 12613-12618.	1.7	22

#	Article	IF	CITATIONS
55	Novel crown ether substituted phthalocyanine with good gas sensing properties to NO2. Journal of Materials Chemistry, 1999, 9, 1415-1418.	6.7	21
56	Flexible, ambipolar organic field-effect transistors based on the solution-processed films of octanaphthoxy-substituted bis(phthalocyaninato) europium. Dyes and Pigments, 2015, 115, 67-72.	2.0	19
57	Functionalized CNTs as Effective Additives to Improve the Efficiency of Perovskite Solar Cells. ACS Applied Energy Materials, 2020, 3, 11674-11680.	2.5	19
58	Enhanced Performance and Stability of Planar Perovskite Solar Cells by Interfacial Engineering using Fluorinated Aliphatic Amines. ACS Applied Energy Materials, 2019, 2, 6230-6236.	2.5	18
59	High-performance and wearable hazardous gases sensor based on n-n heterojunction film of NGO and tetrakis(1-pyrenyl)porphyrin. Journal of Hazardous Materials, 2021, 419, 126460.	6.5	18
60	Turning built-in electric field of porphyrin on Ti3+ self-doped blue-TiO2 hollow nanospheres boosts peroxidase-like activity for high-performance biosensing. Chemical Engineering Journal, 2022, 441, 136070.	6.6	18
61	Spectroscopic and structural characteristics of Langmuir–Blodgett films of bis[2,3,9,10,16,17,24,25-octakis(octyloxy)phthalocyaninato] rare earth complexes. Thin Solid Films, 2006, 496, 619-625.	0.8	16
62	Amphiphilic unsymmetrically substituted porphyrin zinc derivatives: synthesis, aggregation behavior of the self-assembled films and NO ₂ sensing properties. New Journal of Chemistry, 2016, 40, 3323-3329.	1.4	16
63	Highly selective room-temperature NO ₂ sensors based on a fluoroalkoxy-substituted phthalocyanine. New Journal of Chemistry, 2018, 42, 6713-6718.	1.4	16
64	Controlled morphology of self-assembled microstructures via solvent-vapor annealing temperature and ambipolar OFET performance based on a tris(phthalocyaninato) europium derivative. Dyes and Pigments, 2017, 143, 203-210.	2.0	15
65	Diverse sensor responses from two functionalized tris(phthalocyaninato)europium ambipolar semiconductors towards three oxidative and reductive gases. Journal of Materials Chemistry C, 2019, 7, 424-433.	2.7	15
66	Ambipolar chemical sensors based on the self-assembled film of an amphiphilic (phthalocyaninato) (porphyrinato) europium complex. Inorganic Chemistry Communication, 2017, 86, 1-5.	1.8	14
67	Porphyrin polymer-derived single-atom Fe assisted by Fe2O3 with oxygen vacancy for efficient oxygen reduction reaction. Applied Surface Science, 2022, 592, 153301.	3.1	14
68	Highly selective enzymatic-free electrochemical sensor for dopamine detection based on the self-assemblied film of a sandwich mixed (phthalocyaninato) (porphyrinato) europium derivative. Journal of Porphyrins and Phthalocyanines, 2017, 21, 796-802.	0.4	13
69	Dimeric phthalocyanine-involved double-decker complex-based electrochemical sensor for simultaneous detection of acetaminophen and ascorbic acid. Journal of Materials Science: Materials in Electronics, 2019, 30, 1976-1983.	1.1	12
70	Arrangement of tris(phthalocyaninato) gadolinium triple-decker complexes with multi-octyloxy groups on water surface. Journal of Colloid and Interface Science, 2006, 303, 256-263.	5.0	11
71	High-performance room-temperature NO2 sensors based on microstructures self-assembled from n-type phthalocyanines: Effect of fluorine–hydrogen bonding and metal–ligand coordination on morphology and sensing performance. Organic Electronics, 2017, 50, 389-396.	1.4	11
72	Synthesis, fabrication of self-assembled film and ambipolar chemical sensing properties of triple-decker (phthalocyaninato) (porphyrinato) europium complex. Journal of Porphyrins and Phthalocyanines, 2017, 21, 893-899.	0.4	10

#	Article	IF	CITATIONS
73	A novel calix[4]arene-modified porphyrin-based dual-mode sensor for the specific detection of dopamine with excellent performance. New Journal of Chemistry, 2019, 43, 10376-10381.	1.4	10
74	Crystallization Kinetics Engineering toward High-Performance and Stable CsPbBr ₃ -Based Perovskite Solar Cells. ACS Applied Energy Materials, 2021, 4, 10610-10617.	2.5	10
75	Inspired from Spiro-OMeTAD: developing ambipolar spirobifluorene derivatives as effective passivation molecules for perovskite solar cells. Journal of Materials Chemistry C, 2022, 10, 1357-1364.	2.7	10
76	2,3,9,10,16,17,23,24-Octakis(phenoxy/octyloxy)phthalocyaninato manganese complexes. Synthesis, structure, and nonlinear optical property. Dyes and Pigments, 2013, 99, 154-159.	2.0	9
77	A sandwich-type tetrakis(phthalocyaninato) europium–cadmium quadruple-decker complex: structural, spectroscopic, OFET, and gas sensing properties. New Journal of Chemistry, 2019, 43, 15763-15767.	1.4	9
78	A calix[4]arene-modified (Pc)Eu(Pc)Eu[T(C4A)PP]-based sensor for highly sensitive and specific host–guest electrochemical recognition. Dalton Transactions, 2019, 48, 718-727.	1.6	9
79	A phthalocyanine sensor array based on sensitivity and current changes for highly sensitive identification of three toxic gases at ppb levels. New Journal of Chemistry, 2020, 44, 13240-13248.	1.4	9
80	Hierarchical Selfâ€Assembly of Tetrakis(1â€pyrenyl)porphyrins into Microscopic Petals and Flowers with Ultrasensitive Roomâ€Temperature NO ₂ Sensing in a Broad Humidity Range. ChemNanoMat, 2019, 5, 1408-1417.	1.5	8
81	Fine-Tuning Intermolecular and Intramolecular Interactions to Build the Films of Tris(Phthalocyaninato) Rare Earth Complexes and Their Comparative Performances in Ambipolar Gas Sensing. IEEE Transactions on Electron Devices, 2019, 66, 1930-1936.	1.6	8
82	Modifying perovskite solar cells with l(+)-cysteine at the interface between mesoporous TiO2 and perovskite. Sustainable Energy and Fuels, 2020, 4, 878-883.	2.5	8
83	Improved Perovskite/Carbon Interface through Hot-Pressing: A Case Study for CsPbBr ₃ -Based Perovskite Solar Cells. ACS Omega, 2022, 7, 16877-16883.	1.6	8
84	Advances in gas sensors of tetrapyrrolato-rare earth sandwich-type complexes — CommemoratingÂtheÂ100thÂanniversaryÂofÂtheÂbirthÂofÂAcademicianÂGuangxianÂXu. Journal of Rare Earths, 2021, 39, 113-120.	2.5	7
85	Co ₂ O ₃ /Co ₂ N _{0.67} nanoparticles encased in honeycomb-like N, P, O-codoped carbon framework derived from corncob as efficient ORR electrocatalysts. RSC Advances, 2021, 12, 207-215.	1.7	7
86	Surface Modification of Methylamine Lead Halide Perovskite with Aliphatic Amine Hydroiodide. Langmuir, 2018, 34, 9507-9515.	1.6	6
87	Solution-processable (Pc′)Eu(Pc′)Eu[TP(OH)PP]/rGO bilayer heterojunction organic transistors with exceptional excellent ambipolar performance. Journal of Materials Science: Materials in Electronics, 2019, 30, 12437-12446.	1.1	6
88	An Excellent Fe, N Coâ€Doped Porous Biomass Carbon Oxygen Reduction Reaction Electrocatalyst: Effect of Zincâ€Based Activators on Catalytic Activity. Energy Technology, 2020, 8, 2000625.	1.8	6
89	A "micropores & active species protection―strategy for the preparation of a high-performance Fe/S/N-composited porous carbon catalyst for efficient oxygen reduction reaction and zinc–air batteries. Sustainable Energy and Fuels, 2021, 5, 5184-5192.	2.5	6
90	A facile iron-sulfur double-doping strategy to prepare high performance FeNx/S-NC electrocatalyst for oxygen reduction reaction in zinc-air battery. Applied Surface Science, 2022, 580, 152255.	3.1	6

#	Article	IF	CITATIONS
91	Singlet fission in colloid nanoparticles of amphipathic 9,10-bis(phenylethynyl)anthracene derivatives. Journal of Photochemistry and Photobiology A: Chemistry, 2022, 427, 113826.	2.0	6
92	Photoinduced electron and energy transfer in an amphiphilic perylenetetracarboxylic diimide derivative/CdS self-assembled hybrid film. Inorganic Chemistry Communication, 2018, 95, 1-7.	1.8	5
93	Excellent ambipolar gas sensing response of Eu[Pc(OC ₄ H ₉) ₈] ₂ /acidified multiwalled carbon nanotubes hybrid at room temperature. Journal of Porphyrins and Phthalocyanines, 2019, 23, 1455-1462.	0.4	5
94	High mobility at the interface of the cocrystallized sandwich-type tetrapyrrole metal compound and fullerene layers. Inorganic Chemistry Frontiers, 2019, 6, 3345-3349.	3.0	5
95	Ethylthio-substituted sandwich phthalocyaninato europium (III) semiconductors for sensing NO2 and NH3: Effect of the extended π-conjugate systems on tuning the conductivity and sensing behavior. Organic Electronics, 2021, 93, 106151.	1.4	5
96	A voltammetry biosensor based on self-assembled layers of a heteroleptic tris(phthalocyaninato) europium triple-decker complex and tyrosinase for catechol detection. Enzyme and Microbial Technology, 2020, 139, 109578.	1.6	5
97	Design, synthesis, and aggregation behavior of sandwich mixed (phthalocyaninato)(porphyrinato) europium triple-deckers: Effect of substituent on tuning the intermolecular interaction. Inorganic Chemistry Communication, 2015, 54, 50-53.	1.8	4
98	Tuning Semiconductor Performance of Nickel Complexes through Crystal Transformation. Inorganic Chemistry, 2018, 57, 12683-12689.	1.9	3
99	Crown-ether-substituted asymmetric phthalocyanine derivatives/CdS self-assembled hybrid films with an unprecedented high response toward NO2. Journal of Porphyrins and Phthalocyanines, 2019, 23, 507-517.	0.4	3
100	An Activatable Triplet Sensitizer Based on Triplet Electron Transfer and Its Application for Triplet–Triplet Annihilation Upconversion. Journal of Physical Chemistry B, 2020, 124, 6389-6397.	1.2	3
101	Electronic Band Structure Engineering of Transition Metal Oxideâ€N,Sâ€Doped Carbon Catalysts for Photoassisted Oxygen Reduction and Oxygen Evolution Catalysis. Advanced Materials Interfaces, 0, , 2101386.	1.9	3
102	Linker dependent symmetry breaking charge separation in 9,10-bis(phenylethynyl)anthracene dimers. Materials Chemistry Frontiers, 2022, 6, 707-717.	3.2	3
103	Tetrakis(phthalocyaninato) terbium–cadmium quadruple-decker liquid crystals with good semiconducting properties. Organic Electronics, 2014, 15, 2654-2660.	1.4	2
104	Photoinduced electron transfer for improved FET performance based on the hybrid film of an amphiphilic perylene diimide and CdS. Inorganic Chemistry Communication, 2021, 132, 108829.	1.8	2
105	Controlled Preparation and Anti‣ulfate Electrocatalysis of Selfâ€Assembled Multidimensional PtZn Quasiâ€Cubic Nanodendrites. Advanced Materials Interfaces, 0, , 2101944.	1.9	1
106	Efficient singlet fission in nanoparticles of amphipathic anthracene–tetracene dyad with broadband light harvesting ability. Journal of Materials Chemistry C, 2022, 10, 1878-1886.	2.7	1
107	High-selective room-temperature NO2 sensors based on a coumarin-substituted tris(phthalocyaninato) europium. Journal of Porphyrins and Phthalocyanines, 0, , A-G.	0.4	0
107		0.4	0